Title
Understanding order in compositionally graded ferroelectrics: Flexoelectricity, gradient, and depolarization field effects

Journal
Physical Review B, 89(22)

ISSN
2469-9950

Authors
Zhang, J
Xu, R
Damodaran, AR
et al.

Publication Date
2014-06-01

DOI
10.1103/physrevb.89.224101

Peer reviewed

Understanding order in compositionally graded ferroelectrics: Flexoelectricity, gradient, and depolarization field effects

J. Zhang,[1] R. Xu,[1] A. R. Damodaran,[1] Z.-H. Chen,[1] and L. W. Martin[1,2,*]
[1]*Department of Materials Science and Engineering and Materials Research Laboratory, University of Illinois, Urbana-Champaign, Urbana, Illinois 61801, USA*
[2]*Department of Materials Science and Engineering, University of California, Berkeley, Berkeley, California 94720, USA*
(Received 6 April 2014; revised manuscript received 23 May 2014; published 13 June 2014)

A nonlinear thermodynamic formalism based on Ginzburg-Landau-Devonshire theory is developed to describe the total free energy density in (001)-oriented, compositionally graded, and monodomain ferroelectric films including the relative contributions and importance of flexoelectric, gradient, and depolarization energy terms. The effects of these energies on the evolution of the spontaneous polarization, dielectric permittivity, and the pyroelectric coefficient as a function of position throughout the film thickness, temperature, and epitaxial strain state are explored. In general, the presence of a compositional gradient and the three energy terms tend to stabilize a polar, ferroelectric state even in compositions that should be paraelectric in the bulk. Flexoelectric effects produce large built-in fields which diminish the temperature dependence of the polarization and susceptibilities. Gradient energy terms, here used to describe short-scale correlation between dipoles, have minimal impact on the polarization and susceptibilities. Finally, depolarization energy significantly impacts the temperature and strain dependence, as well as the magnitude, of the susceptibilities. This approach provides guidance on how to more accurately model compositionally graded films and presents experimental approaches that could enable differentiation and determination of the constitutive coefficients of interest.

DOI: 10.1103/PhysRevB.89.224101 PACS number(s): 77.22.Ch, 77.22.Ej, 77.55.fe, 77.55.Kt

I. INTRODUCTION

Compositionally graded ferroelectrics possess a spatial variation in chemical composition that breaks the symmetry of the system. In contrast to their homogeneous counterparts, compositionally graded ferroelectrics exhibit self-poling [1], built-in potentials [2], asymmetric or shifted hysteresis loop [3], and the potential for geometric frustration [4]. Their distinctive electric-field, thermal, and stress susceptibilities make such systems potentially important for a range of devices [2]. Compositionally graded ferroelectrics have been probed both experimentally [3,5–8] and theoretically using Slater models [9], phenomenological Landau theory [10–13], transverse Ising models [14,15], and first-principles calculations [4] in an attempt to understand their internal crystal and polarization structure and the mechanisms underlying the manifestation of exotic properties. In this work, we focus on phenomenological approaches and thus narrow our discussion in this capacity.

In general, Ginzburg-Landau-Devonshire (GLD) phenomenological theory expresses the total free energy in terms of the order parameter; for ferroelectrics, this is the electric dipole moment or polarization. GLD theory has been successfully applied in homogeneous bulk [16–19] and thin-film [20,21] ferroelectrics to explore possible crystal and domain structures, electric-field, thermal, stress, and other susceptibilities, as well as chemical, strain, and other perturbations to these materials. Particularly fruitful has been the combination of advanced GLD models with recent developments in the growth of ferroelectric thin films which has enabled unprecedented study of model versions and understanding of the fundamental physics of these materials [22–25]. This also includes the ability to produce deterministically controlled gradients of physical quantities such as strain and composition in ferroelectric films [1,6,8,26–28]. In order to account for the resulting spatial asymmetries that form in these graded films, researchers have suggested the possible inclusion of a number of additional energy terms to adapt such phenomenological models, including (1) flexoelectric, (2) gradient, and (3) depolarization energies [3,10,29,30]. The relative importance, and necessity, of each of these three energies has not, however, been fully considered. In this work, we explore the relative merits, and role, of each of these energies in describing the response of compositionally graded ferroelectric thin films.

The first energy to be considered in this work is the flexoelectric energy. Flexoelectricity is a property of all insulators whereby they polarize when subject to an inhomogeneous deformation [31]. It is expressed as a linear polarization in response to a strain gradient $P_l = \mu_{ijkl}(\partial u_{ij}/\partial x_k)$ where μ_{ijkl} is the flexoelectric polarization coefficient [32–34] which is a fourth-rank tensor, u_{ij} is the strain, and x_k is the position coordinate. The second energy to be considered is the gradient energy. In general, gradient energy arises from spatially inhomogeneous distributions of polarization in a ferroelectric [35]. Typically, it is expressed as the interaction energy per unit volume $g_{ij}(\nabla P)^2$, where g_{ij} is the gradient energy coefficient (which can be directly related to the vibrational spectrum of the crystal) [35]. The final energy to be considered here is the depolarization energy. The depolarization energy can be expressed as $-\frac{1}{2}E_dP$ where E_d is the depolarization field. The depolarization energy arises from a nonvanishing electric field, the so-called depolarization field, inside the ferroelectric that is opposite to the polarization [36].

In this work, we perform a comprehensive study of the effects of flexoelectric, gradient, and depolarization energies on the evolution of polarization and the dielectric and pyroelectric properties in (001)-oriented, monodomain, compositionally graded $Ba_{1-x}Sr_xTiO_3$ ferroelectric films using a GLD

*lwmartin@berkeley.edu

formalism. This study reveals that flexoelectricity produces large built-in fields that work to diminish the temperature dependence of the polarization, dielectric permittivity, and pyroelectric coefficient. We further consider gradient energy terms to represent short-scale correlation between dipoles throughout the smoothly varying film thickness and find that this term has minimal impact on the evolution of polarization and susceptibilities. The depolarization energy is found to give rise to significant differences in the temperature and strain dependence of the susceptibilities in the films. Overall, by first assessing the relative importance of each energy individually, we are able to assess the relative orders of magnitude of coefficients required to induce large effects, provide guidance for the design of experimental approaches to extract the sometimes poorly known coefficients and magnitudes for these effects, and, ultimately, develop a more accurate overall phenomenological model for compositionally graded films.

II. THEORY

A. GLD formalism for homogeneous ferroelectric thin films

Here, we lay the groundwork for the development of a GLD formalism for compositionally graded thin films by first considering homogeneous (001)-oriented, monodomain, epitaxial ferroelectric $BaTiO_3$ and $Ba_{0.6}Sr_{0.4}TiO_3$ films which possess a paraelectric-to-ferroelectric transition between the cubic ($Pm\bar{3}m$) and tetragonal ($P4mm$) phases on a thick substrate under short-circuit boundary conditions. To study $BaTiO_3$, consistent with prior studies [37,38], we have utilized a formalism expanded to the eighth order to account for all possible monodomain phases in the $BaTiO_3$ phase diagram within the temperature range we will consider. To study $SrTiO_3$, again consistent with prior work [39], we have utilized a formalism expanded to the fourth order to include all possible monodomain phases in the $SrTiO_3$ phase diagram within the temperature range we will consider. Considering the mechanical boundary conditions for this situation [i.e., equal in-plane biaxial stress components (in Voigt notation) ($\sigma_1 = \sigma_2$), no shear stresses ($\sigma_4 = \sigma_5 = \sigma_6 = 0$), and no out-of-plane stress ($\sigma_3 = 0$)], the free-energy density for the homogeneous epitaxial ferroelectric films after the necessary Legendre transformation is

$$G_{\text{uni}} = G_0 + \tilde{\alpha}_1 P^2 + \tilde{\alpha}_{11} P^4 + \alpha_{111} P^6 + \alpha_{1111} P^8 + \frac{u_m^2}{s_{11} + s_{12}} - E_{\text{ext}} P, \quad (1)$$

with modified dielectric stiffness coefficients given by [21,40]

$$\tilde{\alpha}_1 = \alpha_1 - \frac{2Q_{12}}{s_{11} + s_{12}} u_m, \quad (2)$$

$$\tilde{\alpha}_{11} = \alpha_{11} + \frac{Q_{12}^2}{s_{11} + s_{12}}, \quad (3)$$

where P is the polarization along the [001], E_{ext} is the external applied electric field (oriented parallel to the polarization direction), α_1, α_{11}, α_{111}, and α_{1111} are dielectric stiffness coefficients, $\alpha_1 = \varepsilon_0(T - T_C)$ (derived from the Curie-Weiss Law) where $\alpha_0 = 1/(2\varepsilon_0 C)$, ε_0 is the permittivity of free space, and C is the Curie-Weiss constant, Q_{ij} are the cubic electrostriction coefficients, and s_{11} and s_{12} are the cubic elastic compliances at constant dielectric displacement. The thermodynamic, elastic, and electromechanical coefficients for $BaTiO_3$ are obtained from Ref. [41] and those of $Ba_{0.6}Sr_{0.4}TiO_3$ are assumed to be a linear function of composition determined by averaging the corresponding values of $BaTiO_3$ and $SrTiO_3$ from Ref. [41] (Table I).

Here, u_m is the in-plane polarization-free misfit strain defined as

$$u_m = \frac{a_{\text{substrate}} - a_{\text{film}}}{a_{\text{film}}}. \quad (4)$$

When the external field $E_{\text{ext}} = 0$, minimization of the total-free-energy density with respect to the polarization ($dG_{\text{uni}}/dP = 0$) yields the spontaneous polarization of the film as a function of the temperature and misfit strain $P_S(T,u_m)$. The lattice parameters a_{film} and $a_{\text{substrate}}$ of $BaTiO_3$, $Ba_{0.6}Sr_{0.4}TiO_3$, and a hypothetical, isotropic substrate are taken to be 0.4005, 0.3965, and 0.3964 nm, respectively, at 25 °C [23,37]. This substrate lattice parameter value was chosen for three reasons: (1) the lattice parameter value is close to that of the commercially available substrate $GdScO_3$, (2) the lattice mismatch between the two end members ($BaTiO_3$ and $Ba_{0.6}Sr_{0.4}TiO_3$) and the substrate is -1.03% and -0.02% (both compressive), respectively, which helps to stabilize the tetragonal phase and enhanced polarization, and (3) the lattice mismatch between the film materials and the substrate are small enough that it should be readily possible to experimentally achieve such structures. Finally, in a compositionally graded film made from these two end member compositions, assuming a coherent strain condition, the strain gradient for the film with a film thickness of 150 nm is 6.67×10^4 m^{-1}.

B. Adapting the formalism for compositionally graded ferroelectric thin films

In this section, we develop the process by which the formalism for homogeneous films is adapted to address compositionally graded versions of ferroelectric films and include details of the selection of the constitutive coefficients used to express the flexoelectric, gradient, and depolarization energy terms.

Flexoelectric coefficient (f_{12}). In general, the flexoelectric coefficients of simple homogeneous insulating solids are quite small, but large flexoelectric coefficients have been reported in several ferroelectric materials [42,43]. In this analysis, the range of flexoelectric coefficients to be considered is obtained by transforming the flexoelectric polarization coefficients (μ_{12}) into flexoelectric strain coefficients (f_{12}) [44] and obtaining both the upper- and lower-bound values from Refs. [42,43]. For simplicity and due to a lack of extensive published data, f_{12} is assumed to be independent of the composition in this case. This is justified since the f_{12} values of $BaTiO_3$ and $Ba_{0.67}Sr_{0.33}TiO_3$ ceramics (at 25 °C) are reported to be very similar (2.899×10^{-9} and 2.739×10^{-9} m^3/C, respectively [42,43]) and thus for simplicity the coefficients are assumed to be constant across the composition range studied. Additionally, the sign of f_{12} is taken as negative, although both positive and negative flexoelectric coefficients have been reported in the literature [42,43,45–47], and for comparison we

TABLE I. Landau coefficients and thermodynamic properties of $BaTiO_3$, $SrTiO_3$, and $Ba_{1-x}Sr_xTiO_3$ (the temperature T in °C) [41].

	$BaTiO_3$	$SrTiO_3$	$Ba_{1-x}Sr_xTiO_3$
a (nm)	0.4005	0.3905	$-0.00995x + 0.40045$
α_1 (10^5 m^2N/C^2)	$4.124(T-115)$	$7.06(T+237.5)$	$56.28(T+352.5x-115)/(-5.7x+13.7)$
α_{11} (10^8 m^6N/C^4)	−2.097	17	$19.1x-2.097$
α_{111} (10^9 $m^{10}N/C^6$)	1.294		$-1.294x+1.294$
α_{1111} (10^{10} $m^{14}N/C^8$)	3.863		$-3.863x+3.863$
Q_{12} (m^4/C^2)	−0.034	−0.0135	$0.0205x-0.034$
s_{11} (10^{-12} m^2/N)	9.1	3.729	$-5.371x+9.1$
s_{12} (10^{-12} m^2/N)	−3.2	−0.9088	$2.291x-3.2$

consider values of $f_{12} = -10^{-10}$, -10^{-9}, and -3×10^{-9} m^3/C in this work.

Gradient energy coefficient (g_{33}). In GLD formalisms for homogeneous ferroelectric films, the order parameter is generally assumed to be a constant throughout the material. This assumption is valid at temperatures far away from T_C, in reasonably thick films, or away from inhomogeneities in the material; however, the fluctuation of the order parameter can become large (i.e., gradient terms become significant) as the temperature approaches T_C, in ultrathin films when surfaces/interfaces come close together, and near inhomogeneities such as domain walls. For a compositionally graded ferroelectric, one might imagine that the magnitude of the polarization (which is directly tied to the composition of the material) could vary throughout the film. The gradient energy term would then work to reduce this variation. For a compositional gradient along the out-of-plane (z) direction, the gradient energy expression reduces to $g_{33}(dP/dz)^2$. The general physical estimation of the gradient coefficient g_{ij} is $g_{ij} \approx \delta^2(T_C/2\varepsilon_0 C)$, where δ is the short-range correlation length that ranges from a few unit cells [35] to a few nanometers [12], and the corresponding order of magnitude of g_{ij} is calculated to be 10^{-12}–10^{-8} m^3V/C. Thus, in this analysis we explore a range of gradient energy coefficients including $g_{33} = 10^{-10}$, 10^{-9}, and 10^{-8} m^3V/C (which are, again, assumed to be independent of the composition).

Depolarization energy and effective permittivity (ε_d). For homogeneous ferroelectric films, the effects of the depolarization field (E_d) are typically found only near the film/contact interface [36,48] where incompletely compensated charge results in an inhomogeneous polarization. In this study, the depolarization field comes from the variation in polarization of the compositionally graded ferroelectric films, and can potentially exist across the entire film thickness. Early phenomenological studies considered the depolarization field to be proportional to either $1/\varepsilon_0$ [48] or $1/\varepsilon_r\varepsilon_0$ [49–51] and both approaches showed large quantitative differences from the experimental data (e.g., the value of T_C from the models can be many times smaller than the values from measurements [52]). In general, the physical justification for these approaches was not provided. Later studies, however, suggested instead that the depolarization field should be proportional to $1/\varepsilon_b$ (a so-called background permittivity) since the order parameter is not only attributed to the soft mode, but from other optical (so-called hard) modes in the material [52–54], which can potentially be much less than ε_r. Ultimately, what these approaches suggested is that in order to achieve a more reasonable estimate of the depolarization field one needed to account for additional screening mechanisms in the material that could effectively reduce the depolarization field to some extent. Using the concept of background permittivity, subsequent theoretical work has demonstrated better agreement with experimental data, but the value of ε_b utilized has had to be varied in the different calculations to achieve good fits [11,55–57]. Add to this the fact that there are defects and charge carriers that can partially screen and/or compensate the depolarization field in real systems thereby potentially reducing the effect of depolarization fields further [2]. Despite such a possibility being noted, there has been no quantitative study that has tried to address how to include such extrinsic effects into the calculation of depolarization field. Here, we define an effective permittivity parameter (ε_d) which incorporates both the background permittivity and other factors that could partially compensate the depolarization field, and thus explore a range of values for $\varepsilon_d = 1$, 5, 10, and 300 (which are again assumed to be independent of composition).

C. Formalism for compositionally graded ferroelectric thin films

Armed with the various terms we will use to adapt the formalisms for homogeneous films, we now articulate the formalism for compositionally graded thin films. Again, we focus on (001)-oriented, compositionally graded, monodomain epitaxial ferroelectrics created by smoothly varying the composition between $BaTiO_3$ and $Ba_{0.6}Sr_{0.4}TiO_3$ on thick substrates under short-circuit boundary conditions. We note that the assumption of mondomain structure, even for a 150-nm-thick film like those considered herein, is justified based on experimental studies that reveal the ability to produce monodomain films like those modeled in this work [58]. The formalism is generally applicable for all ferroelectrics, not just the compositionally graded $Ba_{1-x}Sr_xTiO_3$, but the assumption of monodomain structures is known to be true for this system in thin-film form. The polarization is assumed to be a function of z, i.e., $P = P(z)$. Under the same electrical and mechanical boundary conditions noted in Sec. II A, the total free energy density, taking into account the flexoelectric, gradient, and depolarization field energies, is expressed as

$$G_{\text{grad}} = \int_V (G_{\text{uni}} + G_f + G_g + G_{ES})dV, \qquad (5)$$

where G_f, G_g, and G_{ES} are the flexoelectric, gradient energy, and the electrostatic energy, respectively, expressed as

$$G_f = f_{12}\left[\sigma\frac{\partial P}{\partial z} - P\frac{\partial \sigma}{\partial z}\right], \tag{6}$$

$$G_g = g_{33}\left(\frac{\partial P}{\partial z}\right)^2, \tag{7}$$

$$G_{ES} = -E_{\text{ext}}P - \frac{1}{2}E_d P, \tag{8}$$

where the depolarizing energy $G_d = -\frac{1}{2}E_d P$ is included in G_{ES}. E_d under short-circuit boundary conditions is expressed as

$$E_d = -\frac{1}{\varepsilon_0\varepsilon_d}\left[P - \frac{1}{h}\int_0^h P\,dz\right], \tag{9}$$

in which ε_d again incorporates aspects of the background permittivity and all other factors that influence the evolution of the depolarization field and h is the thickness of the film (here assumed to be 150 nm). From Eq. (9), it is straightforward to see that as ε_d decreases, the magnitude of E_d increases (in other words the less screening that occurs, the larger the effects of the depolarization field). Substituting Eqs. (6)–(9) into Eq. (5), the total free energy density can be expanded as [10,30]

$$\begin{aligned} G_{\text{grad}} = \int_0^h \Big\{ & G_0 + \tilde{\alpha}_1 P^2 + \tilde{\alpha}_{11} P^4 + \alpha_{111} P^6 \\ & + \alpha_{1111} P^8 + f_{12}\left[\sigma\frac{\partial P}{\partial z} - P\frac{\partial \sigma}{\partial z}\right] \\ & + g_{33}\left(\frac{\partial P}{\partial z}\right)^2 - \frac{1}{2}E_d P - E_{\text{ext}} P \\ & + \frac{u_m^2}{s_{11}+s_{12}}\Big\} dz. \end{aligned} \tag{10}$$

Minimization of Eq. (10) yields the Euler-Lagrange relations as

$$\begin{aligned} \frac{\partial G_{\text{grad}}}{\partial P} - \frac{d}{dz}\left(\frac{\partial G_{\text{grad}}}{\partial(\partial P/\partial z)}\right) = 0, \\ \frac{\partial G_{\text{grad}}}{\partial \sigma} - \frac{d}{dz}\left(\frac{\partial G_{\text{grad}}}{\partial(\partial \sigma/\partial z)}\right) = 0. \end{aligned} \tag{11}$$

From Eqs. (10) and (11), the equations of state for the ferroelectric layer are written as

$$\begin{aligned} & 2\alpha_1 P + 4\alpha_{11} P^3 + 6\alpha_{111} P^5 + 8\alpha_{1111} P^7 \\ & - 4Q_{12}\sigma P - 2f_{12}\frac{\partial \sigma}{\partial z} - 2g_{33}\frac{\partial^2 P}{\partial z^2} \\ & + \frac{1}{2\varepsilon_0\varepsilon_d}\left(P - \frac{1}{h}\int_0^h P\,dz\right) - E_{\text{ext}} = 0, \end{aligned} \tag{12}$$

where

$$\sigma = \frac{1}{s_{11}+s_{12}}\left(u_m - Q_{12}P^2 + f_{12}\frac{\partial P}{\partial z}\right). \tag{13}$$

It is seen from Eq. (13) that the total stress is composed of (1) the lattice mismatch between the film and the substrate, (2) the self-strain from the paraelectric-to-ferroelectric phase transition, and (3) the polarization gradient due to a converse flexoelectric effect. Substituting Eq. (13) into (12), we obtain

$$\begin{aligned} & \left(\frac{2f_{12}^2}{s_{11}+s_{12}} + 2g_{33}\right)\frac{\partial^2 P}{\partial z^2} \\ & = 2\tilde{\alpha}_1 P + 4\tilde{\alpha}_{11} P^3 + 6\alpha_{111} P^5 + 8\alpha_{1111} P^7 \\ & \quad - 4P\frac{Q_{12}f_{12}}{s_{11}+s_{12}}\frac{\partial P}{\partial z} - \frac{2f_{12}}{s_{11}+s_{12}}\left(\frac{\partial u_m}{\partial z} - Q_{12}\frac{\partial P^2}{\partial z}\right) \\ & \quad + \frac{1}{2\varepsilon_0\varepsilon_d}\left(P - \frac{1}{h}\int_0^h P\,dz\right) - E_{\text{ext}}. \end{aligned} \tag{14}$$

Again, it is assumed that the thermodynamic, elastic, and electromechanical coefficients of the compositionally graded $Ba_{1-x}Sr_xTiO_3$ films are a linear function of z determined from a weighted average of the coefficients for $BaTiO_3$ and $SrTiO_3$ given in Sec. II A consistent with prior work [59].

The boundary conditions at the interfaces between the film and the bottom or top electrodes are [11,55]

$$\left[P + \lambda\frac{dP}{dz}\right]_{z=0,h} = 0, \tag{15}$$

where λ is the extrapolation length, which is taken as infinite here. The equilibrium polarization P^0 is determined by solving Eq. (14) numerically. The average polarization is calculated by

$$\langle P\rangle = \frac{1}{h}\int_0^h P^0 dz. \tag{16}$$

The effective pyroelectric coefficient π along [001] under $E_{\text{ext}} = 0$ can be determined through the relation

$$\pi = \frac{\partial\langle P\rangle}{\partial T}, \tag{17}$$

and the small-signal effective relative dielectric permittivity (ε_r) along [001] is expressed as

$$\varepsilon_r = \frac{1}{\varepsilon_0}\frac{\partial\langle P\rangle}{\partial E_{\text{ext}}}, \tag{18}$$

where a small E_{ext} is assumed to be uniformly distributed across the film.

III. RESULTS AND DISCUSSION

Using the methodology described in Sec. II, and taking into account the flexoelectric, gradient, and depolarization energies, we have carried out a numerical calculation to analyze the evolution of polarization, dielectric permittivity, and pyroelectric coefficient of four different heterostructures based on $Ba_{1-x}Sr_xTiO_3$ (and assuming growth on a hypothetical substrate with isotropic in-plane lattice parameters of 0.3964 nm): (1) homogeneous, coherently strained $BaTiO_3$ (henceforth referred to as $BaTiO_3$), (2) homogeneous, coherently strained $Ba_{0.6}Sr_{0.4}TiO_3$ (henceforth referred to as $Ba_{0.6}Sr_{0.4}TiO_3$), (3) compositionally graded, coherently strained $Ba_{1-x}Sr_xTiO_3$ possessing a smooth chemical gradient running from $Ba_{0.6}Sr_{0.4}TiO_3$ to $BaTiO_3$ from film-substrate interface to film surface (henceforth referred to as graded), and (4) compositionally graded, coherently strained $Ba_{1-x}Sr_xTiO_3$ films on a range of other substrates possessing a smooth chemical gradient running from $Ba_{0.6}Sr_{0.4}TiO_3$ to $BaTiO_3$

from film-substrate interface to film surface (henceforth referred to as graded/substrate).

A. Probing spatial and temperature dependence of polarization and individual energy contributions

The room-temperature (25 °C) spontaneous polarization (P_S) as a function of distance from substrate has been calculated for $BaTiO_3$, $Ba_{0.6}Sr_{0.4}TiO_3$, and graded heterostructures (Fig. 1). At room temperature, the $BaTiO_3$ is robustly ferroelectric (as would be expected since the bulk $T_C \approx 130\,^{\circ}C$ and the $Ba_{0.6}Sr_{0.4}TiO_3$ (which has a bulk $T_C \approx -20\,^{\circ}C$ is not ferroelectric even under the application of mild compressive strains). For the $BaTiO_3$ heterostructures, the $P_S \approx 0.3\ C/m^2$ at $T = 25\,^{\circ}C$ (larger than that of bulk $BaTiO_3$, $P_S \approx 0.26\ C/m^2$ at $T = 25\,^{\circ}C$) [37]. In a similar manner, we can calculate the thickness dependence of P_S within the graded heterostructures initially assuming no additional energy terms (i.e., $G_f = 0$, $G_g = 0$, $G_d = 0$) [Fig. 1(a)]. In this case, the film is in a condition such that each discrete level along the z direction is effectively isolated from the material above and below it and the P_S of each discrete level is equal to what is expected in a uniform film of that composition grown on the substrate. This represents one extreme case (albeit a simplified one) that is accessible in the models; however, it does not represent a realistic material.

From there, we can systematically introduce the three additional energy terms of interest to gain insight into the role of those energies in driving the evolution of polarization and properties in a realistic film. First, upon introducing flexoelectric energy [Fig. 1(b)], it is observed that the polar state is stabilized throughout the thickness of the film and, as the magnitude of the flexoelectric coefficient increases in magnitude, the polarization is both enhanced and made more uniform throughout the thickness. Upon activating the gradient energy term [Fig. 1(c)], however, considerably less effect is observed. Increasing the magnitude of the gradient energy term also works to stabilize a polar state throughout the film thickness, but the effect is much smaller than that observed for the flexoelectric effect. Finally, upon activating the depolarization energy [Fig. 1(d)], dramatic changes are observed. Consistent with what would be expected, the depolarization energy works to even out the polarization in the film and as the depolarization gets larger (or the ε_d gets smaller) the polarization profile in the film becomes progressively flatter while the average polarization remains the same. Overall, in a compositionally graded heterostructure, the presence of any of the three additional energy terms of interest tends to stabilize a polar, ferroelectric state in compositions found to possess no P_S in the absence of those energies. Flexoelectric effects drive an increase in the average P_S across the entire film thickness, gradient effects impact the P_S values mainly in the phases with the lowest T_C (i.e., those with increased Sr content), and the depolarization energy maintains the same $\langle P \rangle$, while it works to even out the polarization difference across the film. Recall that from Eq. (9), if the polarization gradient is small (as a result of either a small composition gradient or the presence of a large flexoelectric or gradient energies), the E_d can likely be ignored [10].

From here we examine the evolution of P_S with temperature, again for the $BaTiO_3$, $Ba_{0.6}Sr_{0.4}TiO_3$, and graded heterostructures (Fig. 2). For the $BaTiO_3$ heterostructures, the $T_C \approx 400\,^{\circ}C$ (much larger than the bulk $T_C \approx 130\,^{\circ}C$) as a result of the compressive strain from the substrate is consistent with prior experimental work [37]. For the $Ba_{0.6}Sr_{0.4}TiO_3$ heterostructures, consistent with the prior results, the material

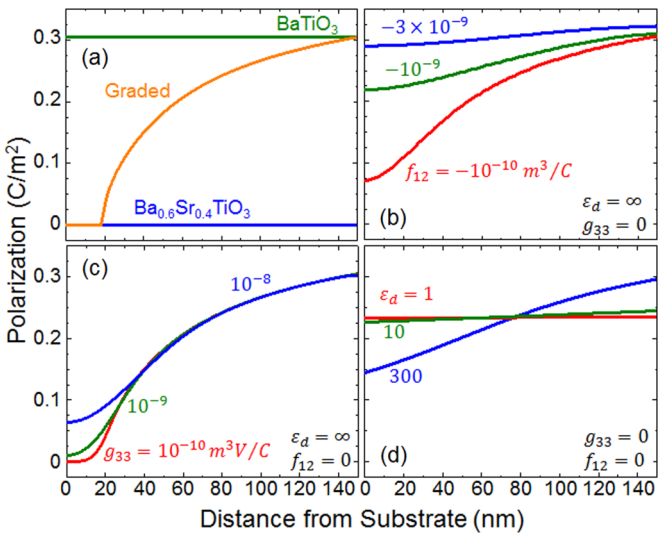

FIG. 1. (Color online) (a) Spontaneous polarization as a function of position throughout the thickness for 150-nm-thick films of $BaTiO_3$ (green), $Ba_{0.6}Sr_{0.4}TiO_3$ (blue), and compositionally graded $BaTiO_3$-$Ba_{0.6}Sr_{0.4}TiO_3$ (orange) under conditions where there are zero flexoelectric, gradient, and depolarization energies. Spontaneous polarization as a function of position throughout the thickness for a 150 nm compositionally graded $BaTiO_3$-$Ba_{0.6}Sr_{0.4}TiO_3$ film under conditions where there is (b) nonzero flexoelectric energy, (c) nonzero gradient energy, and (d) nonzero depolarization energy.

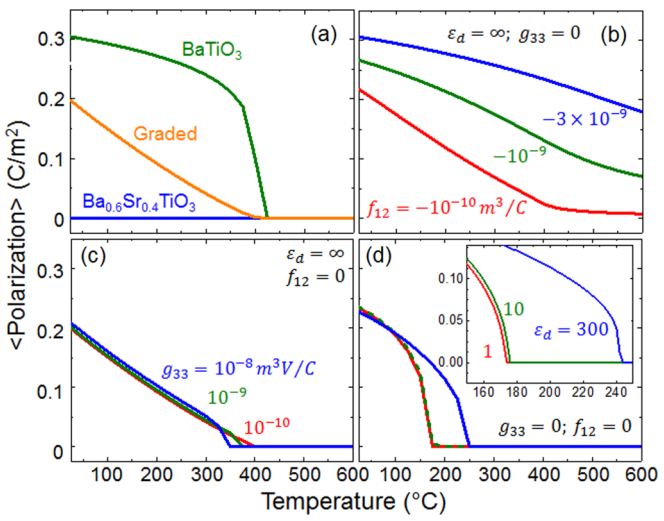

FIG. 2. (Color online) (a) Average polarization as a function of temperature for 150-nm-thick films of $BaTiO_3$ (green), $Ba_{0.6}Sr_{0.4}TiO_3$ (blue), and compositionally graded $BaTiO_3$-$Ba_{0.6}Sr_{0.4}TiO_3$ (orange) under conditions where there are zero flexoelectric, gradient, and depolarization energies. Average polarization as a function of temperature for a 150 nm compositionally graded $BaTiO_3$-$Ba_{0.6}Sr_{0.4}TiO_3$ film under conditions where there is (b) nonzero flexoelectric energy, (c) nonzero gradient energy, and (d) nonzero depolarization energy.

is found to be paraelectric ($P_S = 0$) at and above room temperature even with the application of mild compressive strains. For the graded heterostructures, again initially assuming no additional energy terms (i.e., $G_f = 0$, $G_g = 0$, $G_d = 0$), the overall response is something in-between the case of $BaTiO_3$ and $Ba_{0.6}Sr_{0.4}TiO_3$. The application of a compressive strain from the substrate is found to have a similar effect on the $BaTiO_3$ and lightly Sr-alloyed portions of the films whereby the strain stabilizes ferroelectricity to 400 °C; however, compared to the homogeneous $BaTiO_3$ heterostructure, the $\langle P \rangle$ is systematically lower and undergoes a very broad temperature-dependent change decreasing almost linearly as a function of temperature. In order to differentiate the transition temperature of the graded heterostructures from the T_C of homogeneous films, here we define a T^* to represent the transition temperature where the $\langle P \rangle$ becomes zero.

From there, we can again systematically introduce the three additional energy terms of interest to gain insight into the role of those energies in driving the evolution of $\langle P \rangle$ with temperature in a realistic film. First, upon introducing flexoelectric energy [Fig. 2(b)], we again observe that the presence of a flexoelectric energy works to stabilize a polar, ferroelectric state in the material and that as the flexoelectric coefficient is increased in magnitude, the magnitude of the polarization at all temperatures is seen to increase. In general, the flexoelectric energy is found to operate on the system in much the same way that an externally applied electric field would; it smears out the phase transition and enhances the stability of the polarization. Therefore, in activating a flexoelectric effect, a built-in field, which can be estimated by $E_{flexo} \approx 2 f_{12}(\frac{\partial \sigma}{\partial z})$, is produced in the material. The estimated built-in fields for flexoelectric coefficients $f_{12} = -10^{-10}$, -10^{-9}, and -3×10^{-9} m^3/C are ~30, 300, and 900 kV/cm, respectively. The effect of these built-in fields is essentially equivalent to applying an external electrical field of that same magnitude to the sample and it drives the apparent stabilization and decrease in temperature dependence of the polarization observed here. In general, as the magnitude of f_{12} increases, so does the observed T^*, thus even at temperatures as high as 600 °C, there is a large remnant polarization as a result of the flexoelectric energy term.

Upon activating the gradient energy term [Fig. 2(c)], however, considerably less effect is observed. Again, we consider $g_{33} = 10^{-10}$–10^{-8} m^3V/C and we observe that there is a gradual decrease in T^* and the magnitude of $\langle P \rangle$ near T^* as the magnitude of the gradient energy term is increased. Away from T^* there is almost no change in the $\langle P \rangle$ or its temperature dependence. In fact, even extending this work to explore larger g_{33} coefficients (we explored, but do not show, values as large as 10^{-7} m^3V/C) only changes the T^* value by approximately 50 °C and has little impact on the evolution of polarization away from T^*. Overall, consistent with the studies of the spatial evolution of the polarization, the gradient energy term is found to have minimal impact on the overall response of the material.

Finally, upon activating the depolarization energy [Fig. 2(d)], we again see more dramatic changes in the temperature dependence of $\langle P \rangle$. First, there is a slight enhancement of the $\langle P \rangle$ at room temperature from ~0.2 C/m^2 to ~0.23 C/m^2 just by activating this energy term in any form. Second, T^* is found to decrease as the depolarization energy increases (or the value of ε_d gets smaller). Third, considering that as the depolarization energy increases it has the tendency to even out the polarization of the material, this manifests as a sharpening of the temperature-dependent transition of $\langle P \rangle$. Thus, the curves for systems with larger depolarization energy effects (i.e., those with $\varepsilon_d = 1$ or 10) possess larger values of polarization at low temperatures and smaller values of polarization at higher temperatures near T^* than those systems with reduced depolarization energy effects (i.e., those with $\varepsilon_d = 300$). Finally, and potentially most importantly for experimental study of these materials, is that the magnitude of the depolarization energy manifests itself as a large change (here >65 °C) in the T^* of the system. This provides a direct opportunity for us to extract and better understand the nature of depolarization energy in real systems by carefully measuring the temperature dependence of the polarization.

At this point, it is important to summarize the results thus far that have come from the analyses of the spatial and temperature dependence of the polarization in compositionally graded heterostructures as we systematically activate flexoelectric, gradient, and depolarization energies. First, and most obviously, the larger the magnitude of the coefficient, the more dramatic the effect and change in the properties. Although self-evident, this is important since large error bars on the magnitude of these effects are reported in the literature. Thus, considering a range or working to better quantify these effects is clearly needed to accurately predict the response of such systems. Second, out of the three, the flexoelectric and depolarization energy terms are, in general, found to make considerably larger changes to the spatial and temperature dependence of the polarization than is the gradient energy term. Overall, the flexoelectric energy works to stabilize polar, ferroelectric order, increases the magnitude of the polarization, and gives rise to effects similar to what would be observed under application of an external electric field. Using values of the gradient energy term consistent with those values reported in the literature has minimal effect on these properties, with increasing magnitude resulting in slightly enhanced polarization, but a reduction of the T^* (as if it were trying to homogenize the polar, ferroelectric state). Finally, the depolarization energy term works to homogenize or even out the polarization in the film (while maintaining the $\langle P \rangle$) and increasing the magnitude of this energy term results in what can be large shifts of T^* to lower temperature.

B. Probing the temperature dependence of polarization under the influence of all energies

Armed with the information about how each of the individual energy terms influences the evolution of the P_S and T_C for homogeneous films and $\langle P \rangle$ and T^* for compositionally graded films, we now consider the situation where all the three energies are included in the study of compositionally graded heterostructures. We begin by examining the relative importance and overall effect of the combined energies on the temperature dependence of the $\langle P \rangle$ (Fig. 3). To aid the discussion, we will show three variations in each of which we will hold constant two of the energy terms and vary the third. First, we probe the temperature dependence of

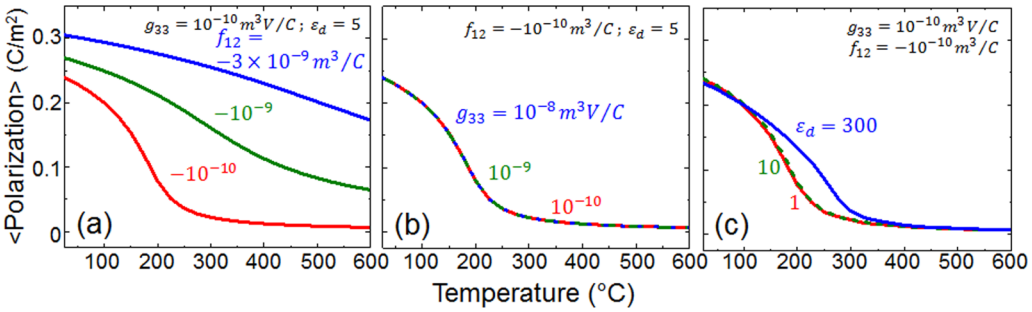

FIG. 3. (Color online) Average polarization as a function of temperature for a 150-nm-thick compositionally graded $BaTiO_3$-$Ba_{0.6}Sr_{0.4}TiO_3$ film under the influence of all three energies of interest with varying (a) flexoelectric, (b) gradient, and (c) depolarization energies.

$\langle P \rangle$ fixing $g_{33} = 10^{-10}$ m^{3}V/C and $\varepsilon_d = 5$ and allowing the magnitude of f_{12} to vary from -10^{-10} to -3×10^{-9} m^3/C [Fig. 3(a)]. The most illuminating comparison of these data is to that in Fig. 2(b) where $g_{33} = 0$ and $E_d = 0$ ($\varepsilon_d = \infty$). The changes in the temperature dependence are subtle but important since both the gradient and (more importantly) the depolarization energy terms work to effectively even out the polarization in the film. The effects of this are not obvious if the flexoelectric coefficient is large [as in this case of the curves for $f_{12} = -3 \times 10^{-9}$ m^3/C in Figs. 2(b) and 3(a)] which are very similar as the flexoelectric energy is large enough to completely overwhelm the other effects. At smaller flexoelectric coefficient values, the added influence of the gradient and depolarization energies are manifested in lower temperature and sharper phase transitions. For instance, for $f_{12} = -10^{-10}$ m^3/C, the inflection point (which is close to T^*) where the slope of $\langle P \rangle$ with respect to T reaches a maximum is observed to shift to lower temperatures by nearly 175 °C when all three energy terms are present as compared to the case of only activating the flexoelectric energy.

In the next case study, we probe the temperature dependence of $\langle P \rangle$ fixing $\varepsilon_d = 5$ and $f_{12} = -10^{-10}$ m^3/C and allowing g_{33} to vary from 10^{-10} to 10^{-8} m^{3}V/C [Fig. 3(b)]. Again, the most illuminating comparison of these data is to that in Fig. 2(c) where $E_d = 0$ ($\varepsilon_d = \infty$) and $f_{12} = 0$. Again, even with the three energies activated in the material, there is essentially no difference between the observed temperature dependence for the $\langle P \rangle$ with varying gradient energy. It should be noted, however, that the shape of the temperature dependence and the effective T^* values do change when the flexoelectric and depolarization energies are turned on. For the combination of flexoelectric and depolarization energy values used here, the temperature-dependent phase transition is found to be sharper in nature and the T^* values are reduced. Overall, the results simply show that within the range of consideration, the change of the magnitude of gradient energy has little effect on the temperature dependence of the $\langle P \rangle$ for the graded heterostructures.

Finally, we probe the temperature dependence of $\langle P \rangle$ fixing $f_{12} = -10^{-10}$ m^3/C and $g_{33} = 10^{-10}$ m^{3}V/C and allowing ε_d to vary from 1 to 300 [Fig. 3(c)]. The most illuminating comparison of these data is to that in Fig. 2(d) where $f_{12} = 0$ and $g_{33} = 0$. Although the overall trends in the variation of T^* are similar with varying ε_d, the sharpness of the phase transition is found to be reduced when all three energies are present. This likely arises from the fact that the flexoelectric energy terms work counter to the depolarization energy, thereby effectively smearing out the polarization profile.

C. Probing the temperature dependence of dielectric and pyroelectric response under the influence of all energies

Having probed the temperature-dependent evolution of the polarization, it is thus useful to explore the effect of compositional gradients and the presence of flexoelectric, gradient, and depolarization energies on the electric-field and thermal susceptibility of the materials. We begin by examining the effective small-field dielectric permittivity (ε_r) [Figs. 4(a)–4(c)]. As is the case in homogeneous ferroelectric films, the permittivity is expected to peak near the phase transition when the material becomes highly susceptible to perturbations with electric field. Thus, recalling the temperature dependence of the $\langle P \rangle$ (Fig. 3), we expect the permittivity to peak and be a maximum at or near the inflection point observed in the $\langle P \rangle$ profile. Following the procedure above, we first probe the temperature dependence of ε_r fixing $g_{33} = 10^{-10}$ m^{3}V/C and $\varepsilon_d = 5$ and allowing the magnitude of f_{12} to vary from -10^{-10} to -3×10^{-9} m^3/C [Fig. 4(a)]. For comparison, we also provide the response for the $BaTiO_3$ heterostructure. Thus, following from the temperature dependence of the $\langle P \rangle$, the permittivity is found to peak at a range of temperatures depending on the magnitude of the flexoelectric coefficient; the larger the flexoelectric coefficient, the higher the temperature of the peak in the permittivity. It is also observed that there is a broadening of the peak in the permittivity and a reduction in the maximum value of permittivity expected as the flexoelectric coefficient gets larger. In general, the presence of the three energies results in a reduction in the magnitude of the response that is predicted to occur as compared to that for a homogeneous $BaTiO_3$ heterostructure (black curve). The mechanism behind this progressive reduction in the maximum value can be found by investigating the permittivity at different z positions inside the compositionally graded heterostructure. Ultimately, the maximum electric-field-dependent response varies with composition in the film and each portion of the film reaches its maximum at a slightly different temperature which manifests itself as a broadened ε_r peak. As the magnitude of the flexoelectric coefficient is increased, this broadening worsens and the response might be considered to be more akin to that in a relaxor ferroelectric as opposed to a traditional ferroelectric and could provide a pathway by which to achieve large, nearly temperature-independent permittivity in materials.

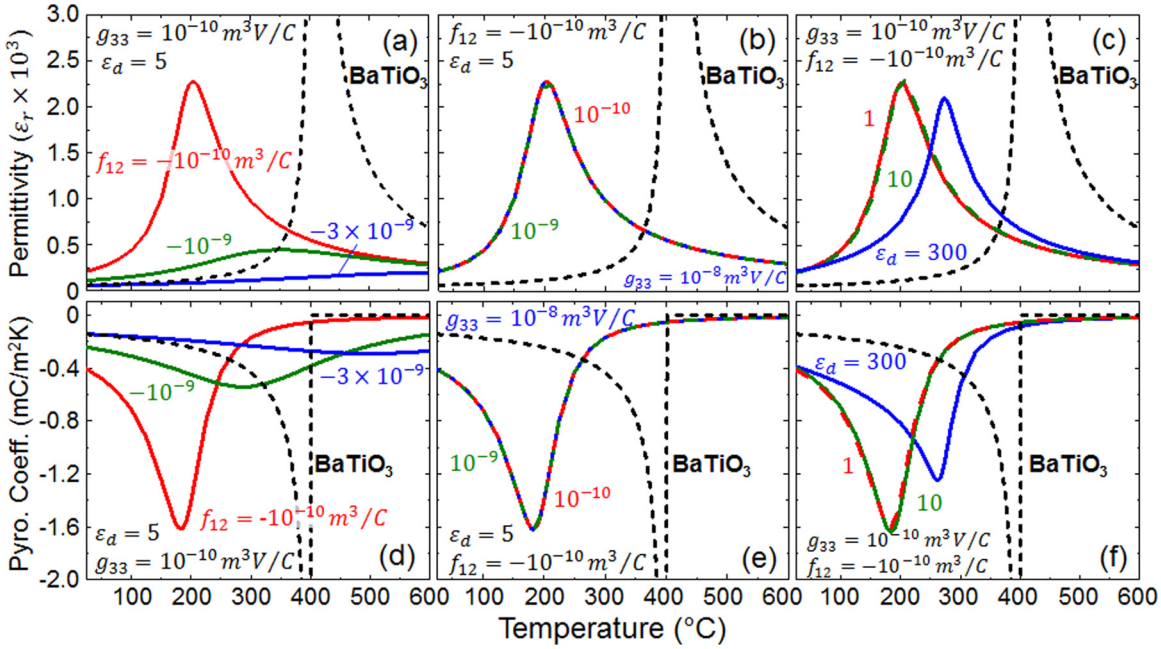

FIG. 4. (Color online) Dielectric permittivity as a function of temperature for a 150 nm compositionally graded $BaTiO_3$-$Ba_{0.6}Sr_{0.4}TiO_3$ film under the influence of all three energies of interest with varying (a) flexoelectric, (b) gradient, and (c) depolarization energies. Effective pyroelectric coefficient as a function of temperature for a 150 nm compositionally graded $BaTiO_3$-$Ba_{0.6}Sr_{0.4}TiO_3$ film under the influence of all three energies of interest with varying (d) flexoelectric, (e) gradient, and (f) depolarization energies. Black data in graphs show a comparison with a coherently strained, homogeneous film of $BaTiO_3$.

In the next case study, we probe the temperature dependence of ε_r fixing $\varepsilon_d = 5$ and $f_{12} = -10^{-10}$ m^3/C and allowing g_{33} to vary from 10^{-10} to 10^{-8} m^{3}V/C [Fig. 4(b)]. As is expected at this point, negligible change in the temperature dependence of ε_r is observed across the range of values studied herein. In general, for the set of energies probed here, there is a reduction in the temperature at which the permittivity is found to peak and in the magnitude of the expected permittivity value. The explanation for such behavior was described in the discussion of the temperature dependence of the $\langle P \rangle$ above. Again, the gradient energy is observed to be less important or impactful than the flexoelectric and depolarization energies at impacting the properties of materials.

Finally, we probe the temperature dependence of ε_r fixing $f_{12} = -10^{-10}$ m^3/C and $g_{33} = 10^{-10}$ m^{3}V/C and allowing ε_d to vary from 1 to 300 [Fig. 4(c)]. Following from the temperature dependence of the $\langle P \rangle$, the permittivity is found to peak at a range of temperatures depending on the magnitude of the depolarization energy term; the larger the depolarization energy (i.e., the smaller ε_d), the higher the temperature of the peak in the permittivity. In general, both the width and maximum value of the peak in permittivity are only weakly dependent on the depolarization energy and are essentially constant for values of $\varepsilon_d < 100$, but are seen to increase in width and decrease in magnitude with $\varepsilon_d > 100$. As the magnitude of the depolarization energy increases (i.e., ε_d gets smaller), the temperature at which the permittivity peaks also decreases. As has been seen in the other cases, the presence of the three energies results in a reduction in the magnitude of the response that is predicted to occur as compared to that for a homogeneous $BaTiO_3$ heterostructure (black curve).

From here, we have also gone on to calculate the effective pyroelectric coefficient (π), calculated at zero applied field, for the graded heterostructures [Figs. 4(d)–4(f)]. For a homogeneous ferroelectric film, π will peak at temperatures close to T_C where the ionic displacement/dipole moments of the ferroelectric become less stable, and a small change in temperature causes a large fluctuation in P_S. For the compositionally graded ferroelectric films, large π will correspondingly occur when there is a large change in the $\langle P \rangle$ with respect to temperature [Eq. (17)]. Thus, following the logic from above and recalling the temperature dependence of the $\langle P \rangle$ (Fig. 3), we expect π to peak and be a maximum at or near the inflection point observed in the $\langle P \rangle$ profile. Again, following the procedure above, we first probe the temperature dependence of π fixing $g_{33} = 10^{-10}$ m^{3}V/C and $\varepsilon_d = 5$ and allowing the magnitude of f_{12} to vary from -10^{-10} to -3×10^{-9} m^3/C [Fig. 4(d)]. Again, for comparison we also provide the response for the $BaTiO_3$ heterostructure. As expected, we observe π to exhibit a maximum value at the observed T^* values and as the flexoelectric coefficient gets larger, the temperature at which this occurs increases (with the maximum occurring at temperatures of $\sim$185 °C, $\sim$290 °C, and $\sim$500 °C for f_{12} values of -10^{-10}, -10^{-9}, and -3×10^{-9} m^3/C, respectively). Likewise, as the flexoelectric coefficient increases in magnitude, a gradual broadening of the phase transition is observed and this results in a systematic reduction in the maximum expected pyroelectric coefficient in the system. Again, this is a potentially important observation. As is the case with permittivity, achieving large, nearly temperature-independent pyroelectric response in materials could have considerable impact on a range of applications.

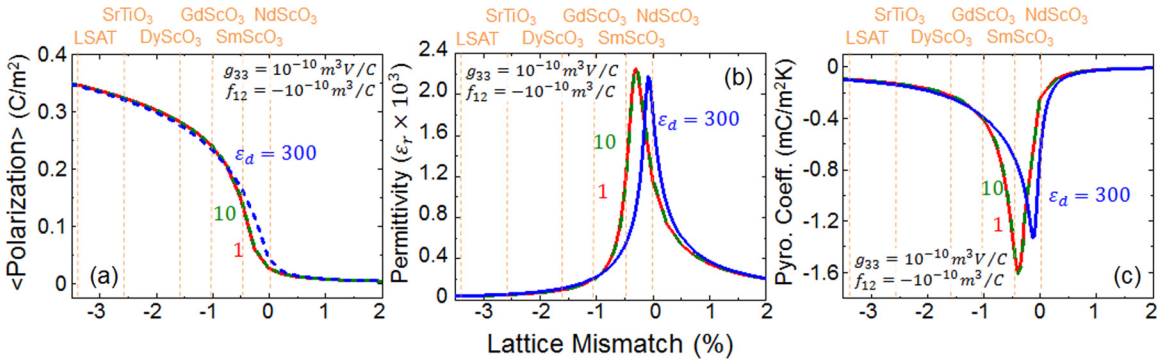

FIG. 5. (Color online) (a) Average polarization, (b) dielectric permittivity, and (c) effective pyroelectric coefficient as a function of epitaxial lattice mismatch for a 150 nm compositionally graded $BaTiO_3$-$Ba_{0.6}Sr_{0.4}TiO_3$ film where $f_{12} = -10^{-10}$ m^3/C, $g_{33} = 10^{-10}$ m^{3}V/C, and ε_d is allowed to vary from 1 to 300. A number of commercially available substrates spanning the range of lattice mismatches studied here are provided for context.

In the next case study, we probe the temperature dependence of π fixing $\varepsilon_d = 5$ and $f_{12} = -10^{-10}$ m^3/C and allowing g_{33} to vary from 10^{-10} to 10^{-8} m^{3}V/C [Fig. 4(e)]. Consistent with prior observations, it is seen that changing the magnitude of the gradient energy has little effect on the temperature dependence of π. Again, the results can be simply understood by revisiting the temperature dependence of the $\langle P \rangle$ [Fig. 3(b)].

Finally, we probe the temperature dependence of π fixing $f_{12} = -10^{-10}$ m^3/C and $g_{33} = 10^{-10}$ m^{3}V/C and allowing ε_d to vary from 1 to 300 [Fig. 4(f)]. Again, for comparison, we also provide the response for the $BaTiO_3$ heterostructure. Consistent with the prior data, the presence of all three energies broadens the temperature dependence and reduces the expected maximum value of π expected for this system. Following from the temperature dependence of the $\langle P \rangle$ [Fig. 3(c)], the π is found to peak at a range of temperatures depending on the magnitude of the depolarization energy term; the larger the depolarization energy (i.e., the smaller ε_d), the lower the temperature of the peak in π. In general, both the width and maximum value of the peak in π are only weakly dependent on the depolarization energy and are essentially constant for values of $\varepsilon_d < 100$, but is seen to increase in width and decrease in magnitude with $\varepsilon_d > 100$.

All told, this study provides important insights into the design of materials to optimize or maximize performance for a given application. It also provides a potential pathway by which it may better quantify our knowledge of flexoelectric coefficients and depolarization energies in materials by fitting experimental data to such curves. Finally, it shows that using compositionally graded thin films, it might be possible to produce materials with large dielectric and/or pyroelectric coefficients which are weakly temperature dependent across large-temperature ranges; this has important implications for a range of applications.

D. Strain dependence of polarization, permittivity, and pyroelectric coefficient under the influence of all energies

Finally, we extend our calculation to consider a wider range of strains and substrates. Thus far, we have examined the effects of flexoelectric, gradient, and depolarization energies on the evolution of polarization, permittivity, and pyroelectric coefficient. To do this, we assumed growth on a hypothetical, isotropic substrate with a similar lattice parameter to $GdScO_3$, but now open up epitaxial strain as an additional variable for study. Here, we will consider strains ranging from -3.5% (compressive) to 2% (tensile) (again assuming a coherently strained film and isotropic in-plane strain) corresponding to the growth on a range of commercially available substrates. To aid the reader, we have labeled six common perovskite-structure substrates as a reference. For brevity, here we show the results of models where $f_{12} = -10^{-10}$ m^3/C and $g_{33} = 10^{-10}$ m^{3}V/C and ε_d is allowed to vary from 1 to 300. The $\langle P \rangle$ reveals a smoothly varying profile, ranging from large values to zero as one transitions from large compressive to large tensile strains [Fig. 5(a)]. There is a rather sharp decrease in the $\langle P \rangle$ in the range -1% to 0% strain, indicative of potential for large susceptibilities in this region. Subsequent calculation of ε_r [Fig. 5(b)] reveals large response in this corresponding strain regime. As the magnitude of the depolarization energy is decreased (i.e., ε_d is increased), the peak in ε_r is found to shift progressively from small compressive strains to nearly zero strain. A similar trend is observed in π [Fig. 5(c)]. This is exciting as thicker films that are coherently strained can be achieved when the lattice mismatch is minimized, thus it might be possible to make high-quality, thick films of coherently strained, compositionally graded $Ba_{1-x}Sr_xTiO_3$ that possess very large dielectric and/or pyroelectric properties.

IV. CONCLUSIONS

In conclusion, we have provided a nonlinear thermodynamic formalism to describe the total free energy density of (001)-oriented, compositionally graded, and monodomain ferroelectric films based on Landau-Ginzburg-Devonshire theory by taking into account flexoelectric, gradient, and depolarization energies. In particular, we have carried out numerical calculations to analyze the effects of each of the three energy components on the evolution of spontaneous polarization, dielectric permittivity, and pyroelectric coefficient as a function of position, temperature, and epitaxial strain state. In general, the presence of the three energies tends to stabilize the polar state in the graded films. Flexoelectric energy results in large built-in fields which diminish the temperature dependence of the polarization, permittivity, and

pyroelectric properties. Gradient energy terms are found to be, compared to both flexoelectric and depolarization energy terms, relatively less important and impactful on the evolution of polarization and properties when considered with reasonable values of the gradient energy coefficient. The depolarization energy, however, is found to play a strong role in the evolution of the polarization and properties. By taking into account the background permittivity and partial screening of the depolarization field, we find that both the position and temperature dependence of the polarization and properties can vary dramatically with changes in depolarization energy which generally attempts to even out the polarization in a graded film. When accounting for all three energies, our studies reveal that the maximum permittivity and pyroelectric coefficients occur under small compressive lattice mismatches, which is exciting since these should be readily achievable in real thin films. Overall, this study provides a generic phenomenological formalism for monodomain, compositionally graded ferroelectric films, offers a more accurate estimation for the nature of response in these materials, and provides practical guidance for how to experimentally address and measure the nature of the various coefficients required to accurately model these materials. Ultimately, compositionally graded thin films represent a stirring new horizon in epitaxial thin-film science and can offer up novel physical phenomena and large susceptibilities that are practically useful if we can better understand and predict how to deterministically control and engineer the gradient structure.

ACKNOWLEDGMENTS

J.Z. and L.W.M. acknowledge support from the Air Force Office of Scientific Research under Grant No. AF FA 9550-11-1-0073 and the Office of Naval Research under Grant No. N00014-10-1-0525. R.X. and L.W.M. acknowledge support from the National Science Foundation and the Nanoelectronic Research Initiative under Grant No. DMR-1124696. A.R.D. and L.W.M. acknowledge support from the National Science Foundation under Grant No. DMR-1149062. Z.H.C. and L.W.M. acknowledge support from the Air Force Office of Scientific Research under Grant No. MURI FA9550-12-1-0471.

[1] J. V. Mantese, N. W. Schubring, A. L. Micheli, and A. B. Catalan, Appl. Phys. Lett. **67**, 721 (1995).
[2] J. V. Mantese and S. P. Alpay, *Graded Ferroelectrics, Transpacitors and Transponents* (Springer, New York, 2005).
[3] J. Karthik, R. V. K. Mangalam, J. C. Agar, and L. W. Martin, Phys. Rev. B **87**, 024111 (2013).
[4] N. Choudhury, L. Walizer, S. Lisenkov, and L. Bellaiche, Nature (London) **470**, 513 (2011).
[5] M. W. Cole, C. V. Weiss, E. Ngo, S. Hirsch, L. A. Coryell, and S. P. Alpay, Appl. Phys. Lett. **92**, 182906 (2008).
[6] R. V. K. Mangalam, J. Karthik, A. R. Damodaran, J. C. Agar, and L. W. Martin, Adv. Mater. **25**, 1761 (2013).
[7] F. Jin, G. W. Auner, R. Naik, N. W. Schubring, J. V. Mantese, A. B. Catalan, and A. L. Micheli, Appl. Phys. Lett. **73**, 2838 (1998).
[8] N. W. Schubring, J. V. Mantese, A. L. Micheli, A. B. Catalan, and R. J. Lopez, Phys. Rev. Lett. **68**, 1778 (1992).
[9] J. V. Mantese, N. W. Schubring, A. L. Micheli, A. B. Catalan, M. S. Mohammed, R. Naik, and G. W. Auner, Appl. Phys. Lett. **71**, 2047 (1997).
[10] Z.-G. Ban, S. P. Alpay, and J. V. Mantese, Phys. Rev. B **67**, 184104 (2003).
[11] M. B. Okatan, A. L. Roytburd, V. Nagarajan, and S. P. Alpay, J. Phys.: Condens. Matter **24**, 024215 (2012).
[12] A. L. Roytburd and J. Slutsker, Appl. Phys. Lett. **89**, 042907 (2006).
[13] S. Zhong, S. P. Alpay, Z.-G. Ban, and J. V. Mantese, Appl. Phys. Lett. **86**, 092903 (2005).
[14] H.-X. Cao and Z.-Y. Li, J. Phys.: Condens. Matter **15**, 6301 (2003).
[15] X. S. Wang, C. L. Wang, W. L. Zhong, and P. L. Zhang, Phys. Lett. A **285**, 212 (2001).
[16] A. F. Devonshire, Philos. Mag. **42**, 1065 (1951).
[17] V. L. Ginzburg, Zh. Eksp. Teor. Fiz. **15**, 739 (1945).
[18] V. L. Ginzburg, Zh. Eksp. Teor. Fiz. **19**, 36 (1949).
[19] M. J. Haun, E. Furman, S. J. Jang, H. A. McKinstry, and L. E. Cross, J. Appl. Phys. **62**, 3331 (1987).
[20] N. A. Pertsev, A. G. Zembilgotov, and A. K. Tagantsev, Phys. Rev. Lett. **80**, 1988 (1998).
[21] S. P. Alpay, I. B. Misirlioglu, A. Sharma, and Z.-G. Ban, J. Appl. Phys. **95**, 8118 (2004).
[22] K. Rabe, C. H. Ahn, and J.-M. Triscone, *Physics of Ferroelectrics a Modern Perspective*, Topics in Applied Physics Vol. 105 (Springer, Berlin, 2007).
[23] D. G. Schlom, L.-Q. Chen, C.-B. Eom, K. M. Rabe, S. K. Streiffer, and J.-M. Triscone, Annu. Rev. Mater. Res. **37**, 589 (2007).
[24] J. Karthik, J. C. Agar, A. R. Damodaran, and L. W. Martin, Phys. Rev. Lett. **109**, 257602 (2012).
[25] J. Karthik, A. R. Damodaran, and L. W. Martin, Phys. Rev. Lett. **108**, 167601 (2012).
[26] M. Brazier, M. McElfresh, and S. Mansour, Appl. Phys. Lett. **72**, 1121 (1998).
[27] M. W. Cole, E. Ngo, S. Hirsch, M. B. Okatan, and S. P. Alpay, Appl. Phys. Lett. **92**, 072906 (2008).
[28] R. V. K. Mangalam, J. C. Agar, A. R. Damodaran, J. Karthik, and L. W. Martin, ACS Appl. Mater. Interfaces **5**, 13235 (2013).
[29] G. Catalan, L. J. Sinnamon, and J. M. Gregg, J. Phys.: Condens. Matter **16**, 2253 (2004).
[30] E. A. Eliseev, A. N. Morozovska, G. S. Svechnikov, P. Maksymovych, and S. V. Kalinin, Phys. Rev. B **85**, 045312 (2012).
[31] P. Zubko, G. Catalan, and A. K. Tagantsev, Annu. Rev. Mater. Res. **43**, 387 (2013).
[32] A. K. Tagantsev, Phys. Rev. B **34**, 5883 (1986).
[33] A. K. Tagantsev, Sov. Phys.–Usp. **30**, 588 (1987).

[34] A. K. Tagantsev, Phase Trans. **35**, 119 (1991).
[35] B. A. Strukov and A. P. Levanyuk, *Ferroelectric Phenomena in Crystals: Physical Foundations* (Springer, Berlin, 1998).
[36] R. R. Mehta, B. D. Silverman, and J. T. Jacobs, J. Appl. Phys. **44**, 3379 (1973).
[37] K. J. Choi, M. Biegalski, Y. L. Li, A. Sharan, J. Schubert, R. Uecker, P. Reiche, Y. B. Chen, X. Q. Pan, V. Gopalan, L. Q. Chen, D. G. Schlom, and C. B. Eom, Science **306**, 1005 (2004).
[38] Y. L. Li and L. Q. Chen, Appl. Phys. Lett. **88**, 072905 (2006).
[39] N. A. Pertsev, A. K. Tagantsev, and N. Setter, Phys. Rev. B **61**, R825 (2000).
[40] J. Zhang, A. A. Heitmann, S. P. Alpay, and G. A. Rossetti, Jr., J. Mater. Sci. **44**, 5263 (2009).
[41] L. Q. Chen, in *Physics of Ferroelectrics a Modern Perspective*, Topics in Applied Physics Vol. 105, edited by K. Rabe, C. H. Ahn, and J.-M. Triscone (Springer, Berlin, 2007).
[42] W. Ma and L. E. Cross, Appl. Phys. Lett. **81**, 3440 (2002).
[43] W. Ma and L. E. Cross, Appl. Phys. Lett. **88**, 232902 (2006).
[44] W. Ma, Phys. Status Solidi B **245**, 761 (2008).
[45] P. V. Yudin and A. K. Tagantsev, Nanotechnology **24**, 432001 (2013).
[46] I. Ponomareva, A. K. Tagantsev, and L. Bellaiche, Phys. Rev. B **85**, 104101 (2012).
[47] R. Maranganti and P. Sharma, Phys. Rev. B **80**, 054109 (2009).
[48] R. Kretschmer and K. Binder, Phys. Rev. B **20**, 1065 (1979).
[49] Q. Zhang and I. Ponomareva, New J. Phys. **15**, 043022 (2013).
[50] Y. Zheng, B. Wang, and C. H. Woo, Appl. Phys. Lett. **88**, 092903 (2006).
[51] S. Choudhury, Y. L. Li, C. E. Krill III, and L.-Q. Chen, Acta Mater. **53**, 5313 (2005).
[52] A. K. Tagantsev, Ferroelectrics **375**, 19 (2008).
[53] A. K. Tagantsev and G. Gerra, J. Appl. Phys. **100**, 051607 (2006).
[54] A. K. Tagantsev, Ferroelectrics **69**, 321 (1986).
[55] J. Hlinka and P. Marton, Phys. Rev. B **74**, 104104 (2006).
[56] B. Winchester, P. Wu, and L. Q. Chen, Appl. Phys. Lett. **99**, 052903 (2011).
[57] D. C. Ma, Y. Zheng, and C. H. Woo, Acta Mater. **57**, 4736 (2009).
[58] A. R. Damodaran, J. Zhang, and L. W. Martin (unpublished).
[59] J. Zhang, M. W. Cole, and S. P. Alpay, J. Appl. Phys. **108**, 054103 (2010).